

Optical Modes in 2-D Imperfect Square and Triangular Microcavities

Svetlana V. Boriskina, *Member, IEEE*, Trevor M. Benson, *Senior Member, IEEE*, Phillip Sewell, *Senior Member, IEEE*, and Alexander I. Nosich, *Fellow, IEEE*

Abstract—Transformation of the whispering-gallery (WG)-modes in imperfect two-dimensional square and triangular microcavities with various degrees of deformation is studied by means of the Muller boundary integral equation technique. Continuous transformation of a circular microcavity, which supports double-degenerate WG-modes, toward a square or a triangle removes the degeneracy of certain WG-modes. The spectrum of the modes that split depends on the symmetry of the emerging microcavity: $WG_{2m,n}$ -modes in case of a C_{4v} symmetry (square) or $WG_{3m,n}$ -modes in the case of C_{3v} symmetry (triangle). In both cases, the modes with the highest Q -factors are nondegenerate modes with antisymmetrical field patterns. We estimate mode frequencies, quality factors and field distributions of practically achievable rather than “ideal” square and triangular microcavities, and compare the effect of various types of fabrication imperfections (corner sharpness, sidewall curvature and surface roughness) on their characteristics. Accurate study of the modal spectra enables us to confirm and explain previous observations, such as: 1) co-existence of the WG-like and volume modes in square microcavities; 2) the separation of the high- Q WG-like modes being twice that determined by the cavity length; and 3) much lower Q -factors of realistic concave-wall triangular microcavities than those of their ideal counterparts.

Index Terms—Mode degeneracy, Muller boundary integral equations (MBIEs), optical microcavities, square resonators, surface roughness, triangular resonators, whispering gallery (WG)-modes.

I. INTRODUCTION

RECENTLY, along with circular microcavities, dielectric and semiconductor cavities of square and triangular shapes [1]–[8] have attracted much interest as light sources and add/drop filters for wavelength-division multiplexing (WDM). They provide directional light emission [1], [6] and more efficient microcavity-to-straight-waveguide coupling than

Manuscript received August 24, 2004; revised February 3, 2005. This work has been supported by the U.K. Engineering and Physical Sciences Research Council (EPSRC) under Grants GR/R90550/01 and GR/S60693/01.

S. V. Boriskina is with the George Green Institute for Electromagnetics Research, School of Electrical and Electronic Engineering, University of Nottingham, Nottingham NG7 2RD, U.K., and also with the School of Radio Physics, Kharkov National University, Kharkov 61077, Ukraine (e-mail: eezsb@gwmail.nottingham.ac.uk).

T. M. Benson and P. Sewell are with the George Green Institute for Electromagnetics Research, School of Electrical and Electronic Engineering, University of Nottingham, Nottingham NG7 2RD, U.K. (e-mail: eeztmb@gwmail.nottingham.ac.uk; eezps@gwmail.nottingham.ac.uk).

A. I. Nosich is with the George Green Institute for Electromagnetics Research, School of Electrical and Electronic Engineering, University of Nottingham, Nottingham NG7 2RD, U.K., and also with the Institute of Radio Physics and Electronics, National Academy of Sciences of Ukraine, Kharkov 61085, Ukraine (e-mail: alex@emt.kharkov.ua).

Digital Object Identifier 10.1109/JQE.2005.846696

conventional circular resonators [2], [3]. To study the optical modal spectra of such resonators, approximate techniques such as ray optics and paraxial approximation are frequently used [1], [6]. Though being useful for studying the characteristics of optically large resonators, they fail to provide reliable results for microcavities whose size is comparable to the wavelength [3]. At the same time, reducing cavity size is crucial for increasing its free spectral range and thus achieving stable single-mode operation. Modern nanofabrication techniques enable realization of ultra-compact microresonators with dimensions comparable to the operating wavelengths.

Mode characteristics of *ideal* (sharp-corner and straight-wall) wavelength-scale square and triangular resonators have been studied extensively by analytical methods and flexible, yet time-consuming, finite-difference-time-domain (FDTD) techniques [4], [5], [7]. However, in many practical cases, cavities are formed with convex sides and rounded corners due to the fabrication process [6], [8]. Such deformed square cavities have been shown to support distorted whispering-gallery (WG)-modes together with the modes associated with the ideal square shape [6]. If a resonator is deformed from the ideal circular, triangular, or square geometry, the analytical methods [4], [5], [7] specifically adapted to model a particular cavity shape cannot provide results with adequate accuracy.

The method of two-dimensional (2-D) Muller boundary integral equations (MBIEs) [9] provides the flexibility to simulate microcavities with smooth contours of *arbitrary* shape. It has already been demonstrated to yield remarkable accuracy and excellent agreement with experimental data for thin microdisks [9]. In this paper, we apply the MBIEs method to the study of the modal spectra of wavelength sized square and triangular microcavities with rounded corners and investigate the transformation of the modes in such cavities with changes in the magnitude of the contour deformation.

II. MODELS OF REALISTIC MICROCAVITIES

The results of previous work aimed at studying the optical spectra of ideal square and triangular microdisks have shown that some modes with high quality factors can be supported in such cavities [4], [5], [7], [9]. However, experimental work revealed that it is very difficult to define sharp corners and straight sidewalls during the fabrication process of optical cavities [6], [8]. Scanning electron microscope photographs of square resonators fabricated using dye-doped organic–inorganic hybrid glass film coating a cross section of a square-shaped fiber (see [6, Fig. 1]) reveal rounded corners and convex sidewalls, and

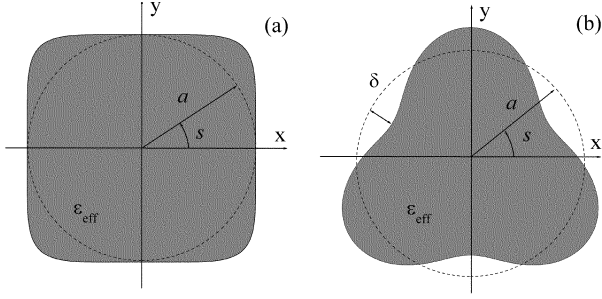


Fig. 1. Schematic diagrams of the cross sections of deformed (a) square and (b) triangular cavities described parametrically by (1)–(3).

other fabrication techniques can yield similar contour deformations of microcavities. For example, it has been observed that semiconductor triangular microcavities fabricated using standard photolithography and two-step inductively coupled plasma etching technique featured rounded vertices and curved sidewalls (see [8, Fig. 1]). Such shape imperfections yielded significantly lower values of cavity mode Q -factors than those predicted for ideal cavities [8]. It should also be noted that the curvature of the sidewalls and corners cannot be replicated precisely and varies from sample to sample. This fact may have two important implications. First, a noticeable frequency shift and Q -factor decrease can occur in some samples, calling for post-fabrication testing and correction of device characteristics. Second, if the cavity shape is close to a circle, then it is possible that such a cavity supports deformed low- Q WG-modes rather than the modes associated with either an ideal square or an ideal triangular resonator.

To study how the change of the resonator sidewall and corner curvature affects its modal characteristics, we describe the smooth cross-sectional contour of the cavity parametrically as follows:

$$\begin{aligned} x &= ar(s) \cos s, & y &= ar(s) \sin s \\ x &= x(s), & y &= y(s), & 0 \leq s \leq 2\pi \end{aligned} \quad (1)$$

where

$$r(s) = (|\cos s|^{2\nu} + |\sin s|^{2\nu})^{-1/2\nu}. \quad (2)$$

The parametric formula (1) together with (2) describes a square with rounded corners and convex sides [Fig. 1(a)], with a value of the curvature at the corners proportional to ν/a . The contour with $\nu = 1$ corresponds to the circle. Increasing the value of ν yields square microcavities with progressively sharper corners and straighter walls. In a similar manner, the function

$$r(s) = 1 + \delta \sin(3s) \quad (3)$$

describes a deformed triangle as shown in Fig. 1(b), with the parameter δ controlling the magnitude of the contour deformation ($\delta = 0$ for the circle).

In the following sections, we shall study the effect of continuous changing the cavity geometry from a circle to a square and a triangle on the transformation of the cavity's optical

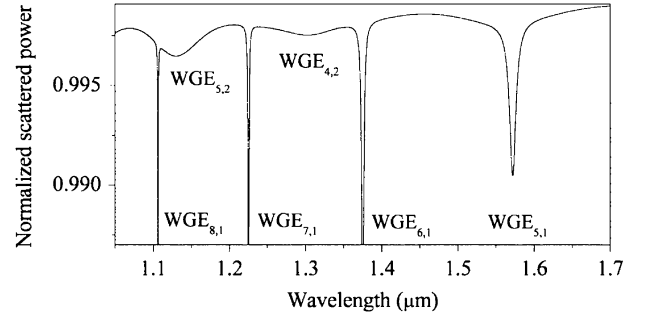


Fig. 2. Wavelength dependence of the total power scattered from a circular microcavity ($2a = 1.6 \mu\text{m}$, $\epsilon_{\text{eff}} = 6.9169 + i10^{-4}$) excited by a TE-polarized CPS beam ($kb = 10$, $\beta = 170^\circ$, $kx_0 = ka + kb + 0.1$, $kx_0 = 0$). The minima in the plot are due to the absorption of the beam power in the cavity at the wavelengths corresponding to the excitation of the cavity WG-modes.

mode spectra and estimate the values of practically achievable mode Q -factors. Unlike previously published FDTD data on the square and triangular cavity modes, our results (complex frequencies and modal fields) are obtained with guaranteed four-digit accuracy—thanks to the advanced numerical algorithm published in [9].

III. CIRCULAR MICROCAVITY TE-MODE SPECTRA

For numerical simulation, we reduce the original three-dimensional (3-D) thin microdisk to an equivalent 2-D structure by using the Effective Index method (see, e.g., [9]). The WG-modes of the 2-D circular microcavity are classified as $\text{WGE}(H)_{m,n}$ -modes, m being the azimuthal mode number, and n the radial mode number. As has been experimentally observed [10], in thin circular microdisk resonators, the dominant modes are quasi-TE-polarized $\text{WGE}_{m,1}$ -modes with one radial field variation with the electric field vector mainly in the plane of the disk. These demonstrate the highest Q -factors and strongly modify spontaneous emission in the microdisks. The Q -factors of the dominant $\text{WGE}_{m,1}$ -modes increase exponentially with increasing azimuthal mode number m [11]. The higher order radial modes have lower Q -factors and are usually considered as parasitic. The larger the optical size of the microcavity, the greater the number of higher order WG-modes it supports. More accurately, it has been shown in [12] that, for a given disk, only the modes with azimuthal index m between $2\pi a/\lambda$ and $2\pi a|n_{\text{eff}}|/\lambda$ (n_{eff} is effective refractive index, λ is the wavelength) display the WG behavior with $Q_m \sim e^m$. If $m < 2\pi a/\lambda$, the modes still exist, however their Q -factors are small and $Q_m \sim m^2$. If $m > 2\pi a|n_{\text{eff}}|/\lambda$, natural modes do not exist at all.

The optical spectrum of a circular microcavity with diameter $2a = 1.6 \mu\text{m}$, and effective refractive index $n_{\text{eff}} = 2.63$ is shown in Fig. 2. This effective refractive index corresponds to the propagation constant of the fundamental mode at a wavelength of $1.55 \mu\text{m}$ in an air-clad GaInAsP disk of thickness 200 nm and refractive index of 3.37 . The microcavity is optically excited by a complex point source (CPS) beam (see [9] for details). The beam is focused onto the rim of the cavity to enhance the excitation of the WG-mode resonances. We can clearly observe two families of WGE-modes (of the first and second radial order) that are supported by the cavity in the frequency range

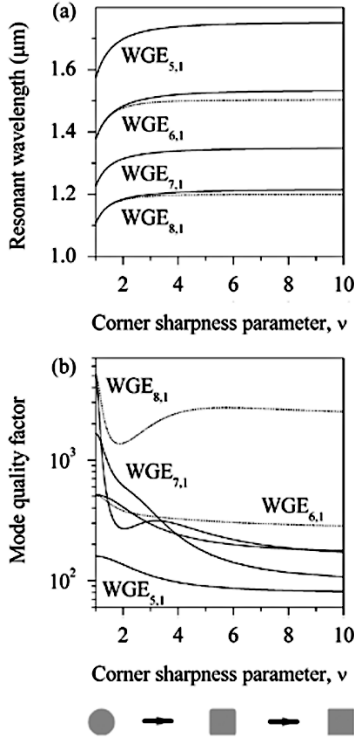


Fig. 3. (a) Shift and splitting of wavelengths and (b) change of quality factors of the $WGE_{m,1}$ -modes ($m = 5 \dots 8$) in a $1.6\text{-}\mu\text{m}$ diameter circular microcavity with permittivity $\epsilon_{\text{eff}} = 6.9169 + i10^{-4}$ transformed into a square one by a continuous change of the corner sharpness parameter ν . The inset shows the cross sections of the cavities with $\nu = 1$, $\nu = 5$, and $\nu = 10$.

considered. All the $WGE_{m,n}$ -modes are double-degenerate due to the circular symmetry of the cavity geometry.

It is known that the spectrum of degenerate and nondegenerate modes supported by an optical resonator is determined by the symmetry of the geometrical structure [13]–[15]. Square microcavities have a C_{4v} symmetry (the structure is invariant under a rotation by $\pi/2$), while triangular resonators have a C_{3v} symmetry (the structure has a $2\pi/3$ rotation invariance). Next, we study the continuous transformation of the circular cavity WG-modes into the modes of the square and triangular microcavities and classify the transformed modes as degenerate pairs and nondegenerate modes. We expect this classification to be helpful in understanding the observed experimental spectra of such resonators.

IV. MODES OF IMPERFECT SQUARE AND TRIANGULAR MICROCAVITIES

A. Square Microcavity

Fig. 3(a)–(b) presents the transformation of the four neighboring first-order WGE-modes shown in Fig. 2 with increasing corner sharpness parameter ν (the lower inset shows the transformation of the cavity contour). One can immediately notice the striking difference in the behavior of the modes with even and odd values of azimuthal mode number. As for the $WGE_{2m+1,1}$ ($m = 0, 1, 2, \dots$)-modes of the circular microcavity, the modes of the square cavity whose indexes sum to an odd number are double-degenerate, and by inspecting their

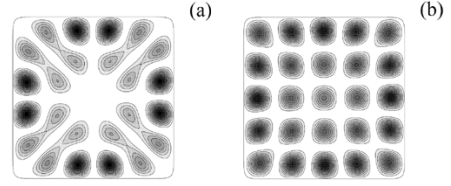


Fig. 4. Magnetic field intensity portraits of (a) symmetrical $TE_{5,5}$ volume mode ($\lambda = 1.215 \mu\text{m}$) and (b) antisymmetrical WG-like mode ($\lambda = 1.119 \mu\text{m}$) of the square microcavity with the side length of $1.6 \mu\text{m}$ and corner sharpness parameter $\nu = 10$. Both modes are nondegenerate and are transformed from the circular-cavity $WGE_{8,1}$ modes of two symmetry types.

field portraits we classified them as $TE_{m,m+1}$ and $TE_{m+1,m}$ volume modes. In contrast, increasing of ν removes the degeneracy of the even m -modes, and they split into two modes, one of which has a much higher value of Q -factor. The near-field portraits of these modes are shown in Fig. 4(a)–(b). The high- Q -mode [Fig. 4(a)] is recognized as the WG-like mode of a square microcavity having an antisymmetrical field pattern with nulls along all four symmetry lines of the square, i.e., along two diagonals and two median lines, or at least along the diagonals. WG-like modes have been studied before, both analytically and numerically, for the cavities with sharp corners [4], [5] and have been found to be the dominant modes of square resonators. They have the highest Q -factors and thus are the most promising for practical applications as optical waveguide filters and microlasers [2]. Because only alternate $WGE_{2m,1}$ -modes split and give rise to the WG-like mode in the square cavity, the square cavity's free spectral range is twice the value determined by the length of its side. The second mode of the split pair [Fig. 4(b)] has a lower Q -factor and a symmetrical field distribution corresponding to that of a $TE_{m,m}$ volume mode.

Furthermore, [see Fig. 3(a)–(b)] the most noticeable shift in wavelength and variation in Q -factor of the WG-like modes occurs over a rather short range of values of the corner sharpness parameter ν ($1 < \nu < 4$). If ν is increased further, the wavelengths do not practically change, and only a slight decrease in Q -factor can be observed. However, as one can see from the inset to Fig. 3, for $\nu = 5$ the cavity is far from the ideal square and has noticeably rounded corners and convex sides. In Fig. 5, we present a comparison of the wavelengths and Q -factors of the modes of the ideal square resonator (computed using the FDTD technique, see [5, Fig. 3(a)]) and the imperfect one with $\nu = 5$. It can be seen (Fig. 5) that the Q -factors of the modes of imperfect square cavities with convex walls and rounded corners can be even higher than those of ideal squares. However, our results show a decrease in the Q -factors of the WG-like modes in the square cavities with concave sidewalls (see Fig. 6).

The preceding observations have the following immediate consequences: 1) although the spectrum of the square resonator is denser than that of a circular cavity of the same size, the spacing of the highest Q modes is twice as large, which is in perfect agreement with the analytical results of [4] and 2) the WG modes demonstrate good stability with respect to the rounded cavity corners and convex cavity sidewalls (the types of fabrication imperfections that frequently occur in square microcavities), and thus square cavities are expected to have high fabrication

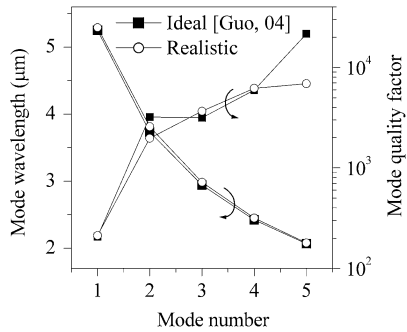


Fig. 5. Mode wavelengths and quality factors of five neighboring TM-polarized WG-like modes in the ideal ([5, Fig. 3(a)] and deformed ($\nu = 5$) square resonators with side length $a = 3 \mu\text{m}$, and effective refractive index $n_{\text{eff}} = 3.2$. In the notation of [5], the modes are $\text{TM}_{0,l}$ ($l = 8, \dots, 16$), they are transformed from the $\text{WGH}_{m,1}$ ($m = 4, \dots, 12$) modes of the circular cavity.

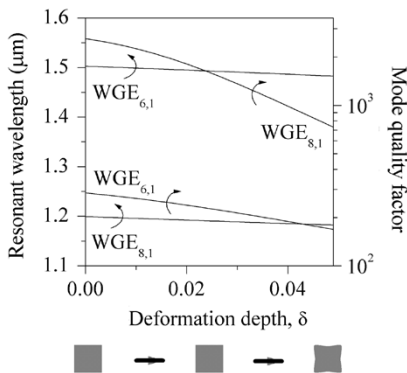


Fig. 6. Wavelengths detuning and quality factors decrease of two WG-like modes in a square microcavity with the same parameters as in Fig. 4 ($\nu = 10$) and concave sidewalls. The cavity shape deformation is described by the following parametric formula: $r(s) = r_{\text{square}}(s) - \delta \cos(4s)$. The inset shows the cross-sections of the cavities with $\delta = 0$, $\delta = 0.025$, and $\delta = 0.05$.

tolerances. All this, together with very efficient ($\sim 75\%$) evanescent-wave coupling to planar waveguides [2], [3], [16] and prisms [17] and the fact that fabrication of square shapes allows better control of sidewall roughness [18] in comparison with circular cavities, makes square resonators promising candidates for single-mode microlasers and filters with stable operation.

B. Triangular Microcavity

We now apply the same approach and track the transformation of WG-modes in deformed triangular microcavities with the same material parameters as the previous example. The microcavity shape defined by the parametric formula (3) describes well a practically realized triangular microcavity deformed in the fabrication process (see [8, Fig 1(a)]). Fig. 7 shows the $\text{WGE}_{m,1}$ -mode wavelengths and Q -factors as a function of the parameter δ , which determines the radial depth of the contour perturbation. As for the square microcavity, increasing the contour deformation toward a shape with three symmetry axes leads to degeneracy removal of those modes whose azimuthal mode number is a multiple of three. Fig. 8 shows the magnetic field intensity portraits for the split modes of the two symmetry types transformed from the $\text{WGE}_{6,1}$ -mode of the circular cavity. It can be seen that the higher Q -mode [Fig. 8(a)] has field nulls on the triangle medians (i.e., lines of symmetry), whereas the lower Q -mode has field maxima.

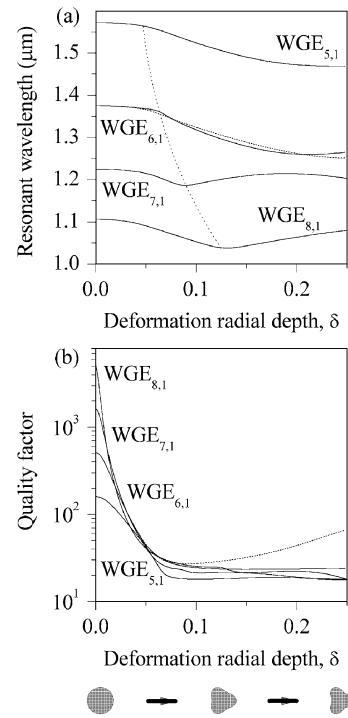


Fig. 7. (a) Shift and splitting of wavelengths and (b) change of quality factors of the $\text{WGE}_{m,1}$ -modes ($m = 5 \dots 8$) in a $1.6\text{-}\mu\text{m}$ -diameter circular microcavity with permittivity $\epsilon_{\text{eff}} = 6.9169 + i10^{-4}$ transformed into a triangular one by a continuous change of the parameter δ . The inset shows the cross section of the cavity for $\delta = 0$, $\delta = 0.175$, and $\delta = 0.25$.

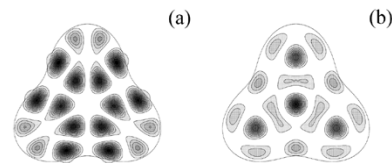


Fig. 8. Magnetic field intensity portraits of two nondegenerate modes of the deformed triangular microcavity ($\epsilon_{\text{eff}} = 6.9169 + i10^{-4}$, $\delta = 0.22$, $a = 0.8 \mu\text{m}$) transformed from the circular-cavity $\text{WGE}_{6,1}$ -modes of two symmetry types: (a) high- Q antisymmetrical mode ($\lambda = 1.255 \mu\text{m}$) and (b) low- Q symmetrical mode ($\lambda = 1.26 \mu\text{m}$).

All the other modes remain double-degenerate, and their Q -factors drastically decrease as the cavity shape tends to that of a deformed triangle. Furthermore, one can note the points on the curves where the mode transformations occur. The points are connected by a dotted line in Fig. 7(a) to demonstrate their migration as the azimuthal order of the WG-mode is increased. It can clearly be seen that the higher the WG-mode azimuthal order, the more stable the mode is with respect to this contour deformation. This is in accordance with the previous observations that high-azimuthal-order WG-modes can survive in extremely deformed elliptical and racetrack resonant cavities [19], [20]. However, the Q -factors of these distorted WG-modes are very low, which renders their application for lasing or filtering impractical.

In Fig. 9, we compare our results for the wavelengths of the TM-polarized modes of the imperfect triangular resonator described by (3) with experimental data and analytical calculations for the corresponding ideal triangular microcavity obtained in [8] (see [8, Figs. 2 and 4]). Although the results obtained for

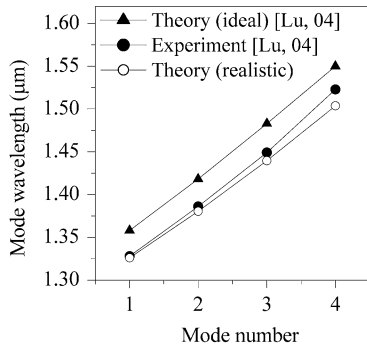


Fig. 9. Comparison of the mode wavelengths of four TM-modes obtained experimentally from the photoluminescence spectrum of a GaInAsP triangular microcavity with side length of $5 \mu\text{m}$ [8]; analytical solutions for the ideal triangle [8]; and numerical solutions for the deformed triangle with $\delta = 0.22$. In our 2-D computations, we used the effective index $n_{\text{eff}} = 3.2$, and $a = 2.29 \mu\text{m}$.

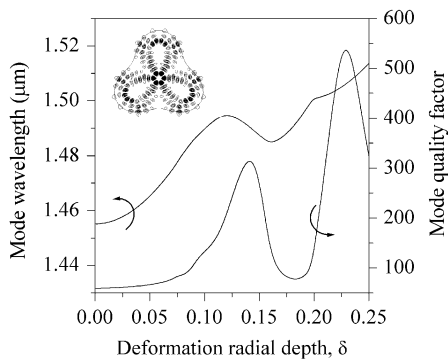


Fig. 10. Mode wavelength and Q -factor of an antisymmetrical TM-mode of the deformed triangular resonator (Mode 4 from Fig. 8) as a function of the deformation radial depth δ . The inset shows the mode electric field intensity portrait in the cavity with $\delta = 0.22$ ($\lambda = 1.504 \mu\text{m}$).

the imperfect resonator contour provide a much better fit to the experimental data, the calculated Q -factors (300–500), even for the imperfect cavity shape, are much larger than those measured in [8] (20–40). To understand which type of fabrication imperfection causes such significant degradation of the Q -factors, we plot in Fig. 10 the dependence of the characteristics of one of the modes (Mode 4) on the value of the parameter δ . This mode is an antisymmetrical nondegenerate mode with the electric field intensity portrait shown in the inset in Fig. 10. We can see that the cavity sidewall curvature has a dominant effect on the mode characteristics as both the modal wavelength and especially the Q -factor can change drastically with even slight changes of this curvature.

C. Sidewall Surface Roughness

Finally, we study the effect of the sidewall surface roughness on the dominant nondegenerate modes in square and triangular microcavities. This type of fabrication imperfection is always present in practical microcavities and can spoil their modal characteristics. It should also be noted here that if modal degeneracy is removed by the imperfect nature of the fabrication process, parasitic modes can appear in the spectra of circular microcavities [21]. However, as the dominant modes in square and triangular resonators are nondegenerate, the sidewall surface roughness due to fabrication errors cannot cause such splitting. We

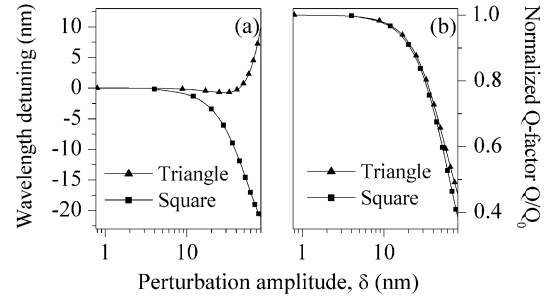


Fig. 11. Wavelength detuning (a) and Q -factor degradation (b) of a WG-like mode of the square microcavity and an antisymmetrical mode of the triangular microcavity (both transformed from the circular-cavity $\text{WGE}_{6,1}$ -mode) as a function of the depth of the sidewall roughness with period $\Lambda = 1/30$. The microcavities have the same parameters as those in Figs. 3 and 7.

have previously shown [22] that low-amplitude surface roughness had minimal effect on the Q -factors of WG-like modes of square microcavities. However, after the roughness amplitude reached a certain threshold value, the Q -factors degraded rapidly.

Following the procedure described in [22], we now study how the presence of the sidewall surface roughness affects the non-degenerate antisymmetric mode of the triangular microcavity. The results for the two cases are compared in Fig. 11, where the same threshold-like behavior of the mode Q -factor is observed with increasing perturbation amplitude. Thus, we can conclude that the low-amplitude sidewall surface roughness practically achievable in modern fabrication techniques is not a dominant mechanism causing degradation of the modal quality factors. However, as we have shown in the previous sections, the sidewall curvature is a parameter that should be controlled precisely in order to achieve high- Q oscillations.

V. CONCLUSION

Continuous transformation of WG-modes of circular resonators into the modes of imperfect square and triangular microcavities has been studied. For the square microcavities, we have shown degeneracy removal for the WG-modes with even azimuthal mode numbers ($\text{WG}_{2m,n}$) and the transformation of the modes with antisymmetrical field patterns into high- Q nondegenerate WG-like modes. This explains a previous observation that the FSR of the WG-like modes in the square microcavity is twice that of the WG-modes in the circular case. In imperfect triangular resonators, the modal degeneracy is removed for the WG-modes whose azimuthal mode number is a multiple of three. The highest Q -modes are again the ones with antisymmetrical field patterns and nulls along all the symmetry axes.

We have estimated the fabrication tolerances of the modes of such microcavities to the contour deformations. Our results show that the square microcavity modes demonstrate good stability with respect to changes in the corner sharpness parameter. Furthermore, their Q -factors can even increase in cavities with rounded corners and convex sides in comparison to those in ideal square resonators. We have also observed that although the modes of both types of cavities are not seriously affected by the low-amplitude surface roughness, they can be quite sensitive to the changes in the sidewall curvature (especially the modes of triangular microresonators).

REFERENCES

- [1] A. W. Poon, F. Courvoisier, and R. K. Chang, "Multimode resonances in square-shaped optical microcavities," *Opt. Lett.*, vol. 26, no. 9, pp. 632–634, Sep. 2001.
- [2] C. Manolatu, M. J. Khan, S. Fan, P. R. Villeneuve, H. A. Haus, and J. D. Joannopoulos, "Coupling of modes analysis of resonant channel add-drop filters," *IEEE J. Quantum Electron.*, vol. 35, pp. 1322–1331, 1999.
- [3] M. Lohmeyer, "Mode expansion modeling of rectangular integrated optical resonators," *Opt. Quantum Electron.*, vol. 34, no. 5/6, pp. 541–557, May/June 2002.
- [4] W.-H. Guo, Y.-Z. Huang, Q.-Y. Lu, and L.-J. Yu, "Whispering-gallery-like modes in square resonators," *IEEE J. Quantum Electron.*, vol. 39, no. 9, pp. 1563–1566, Sep. 2003.
- [5] ———, "Mode quality factor based on far-field emission for square resonators," *IEEE Photon. Technol. Lett.*, vol. 16, no. 2, pp. 479–481, Feb. 2004.
- [6] T. Ling, L. Liu, Q. Song, L. Xu, and W. Wang, "Intense directional lasing from a deformed square-shaped organic-inorganic hybrid glass microring cavity," *Opt. Lett.*, vol. 28, no. 19, pp. 1784–1786, Oct. 2003.
- [7] Y.-Z. Huang, W.-H. Guo, and Q.-M. Wang, "Analysis and numerical simulation of eigenmode characteristics for semiconductor lasers with an equilateral triangle micro-resonator," *IEEE J. Quantum Electron.*, vol. 37, no. 1, pp. 100–107, Jan. 2001.
- [8] Q. Y. Lu, X. H. Chen, W. H. Guo, L. J. Yu, Y. Z. Huang, J. Wang, and Y. Luo, "Mode characteristics of semiconductor equilateral triangle semiconductor microcavities with side length of 5–20 μm ," *IEEE Photon. Technol. Lett.*, vol. 16, no. 2, pp. 359–361, Feb. 2004.
- [9] S. V. Boriskina, P. Sewell, T. M. Benson, and A. I. Nosich, "Accurate simulation of 2-D optical microcavities with uniquely solvable boundary integral equations and trigonometric-galerkin discretization," *J. Opt. Soc. Amer. A*, vol. 21, no. 3, pp. 393–402, Mar. 2004.
- [10] M. Fujita, A. Sakai, and T. Baba, "Ultrasmall and ultralow threshold GaInAsP-InP microdisk injection lasers: Design, fabrication, lasing characteristics, and spontaneous emission factor," *IEEE J. Sel. Topics Quant. Electron.*, vol. 15, no. 3, pp. 673–681, May/June 1999.
- [11] S. L. McCall, A. F. J. Levi, R. E. Slusher, S. J. Pearton, and R. A. Logan, "Whispering-gallery mode microdisk lasers," *Appl. Phys. Lett.*, vol. 60, no. 3, pp. 289–291, Jan. 1992.
- [12] E. I. Smotrova and A. I. Nosich, "Mathematical analysis of the lasing eigenvalue problem for the WG modes in a 2-D circular dielectric microcavity," *Opt. Quantum Electron.*, vol. 36, no. 1–3, pp. 213–221, 2004.
- [13] M. Tinkham, *Group Theory and Quantum Mechanics*, ser. Int. Series in Pure and Applied Physics. New York: McGraw-Hill, 1964.
- [14] S.-H. Kim and Y.-H. Lee, "Symmetry relations of two-dimensional photonic crystal cavity modes," *IEEE J. Quantum Electron.*, vol. 39, no. 9, pp. 1081–1085, Sep. 2003.
- [15] O. Frank and B. Eckhardt, "Eigenvalue density oscillations in separable microwave resonators," *Phys. Rev. E*, vol. 53, no. 4, pp. 4166–4175, Apr. 1996.
- [16] C. Y. Fong and A. W. Poon, "Mode field patterns and preferential mode coupling in planar waveguide-coupled square microcavities," *Opt. Exp.*, vol. 11, no. 22, pp. 2897–2904, Nov. 2003.
- [17] Y.-L. Pan and R. K. Chang, "Highly efficient prism coupling to whispering gallery modes of a square μ cavity," *Appl. Phys. Lett.*, vol. 82, no. 4, pp. 487–489, Jan. 2003.
- [18] L. Bach, A. Wolf, J. P. Reithmaier, and A. Forchel, "Square- and race-track-lasers as active components for monolithically integrated optoelectronic devices," in *Proc. IPRM*, 2002, pp. 111–114.
- [19] S. V. Boriskina, T. M. Benson, P. Sewell, and A. I. Nosich, "Highly efficient design of spectrally engineered whispering-gallery-mode laser resonators," *Opt. Quantum Electron.*, vol. 35, pp. 545–559, Mar./Apr. 2003.
- [20] J. U. Nöckel, A. D. Stone, and R. K. Chang, "Q spoiling and directionality in deformed ring cavities," *Opt. Lett.*, vol. 19, pp. 1693–1695, 1994.
- [21] B. E. Little, J. P. Laine, and S. T. Chu, "Surface-roughness-induced contridirectional coupling in ring and disk resonators," *Opt. Lett.*, vol. 22, pp. 4–6, 1997.
- [22] S. V. Boriskina, T. M. Benson, P. Sewell, and A. I. Nosich, "Spectral shift and Q-change of circular and square-shaped optical microcavity modes due to periodical sidewall surface roughness," *J. Opt. Soc. Amer. B*, vol. 21, no. 10, pp. 1792–1796, Oct. 2004.



Svetlana V. Boriskina (S'96–M'01) was born in Kharkov, Ukraine, in 1973. She received the M.Sc. degree (hons.) in radio physics and the Ph.D. degree in physics and mathematics from Kharkov National University, Kharkov, Ukraine, in 1995 and 1999, respectively.

From 1997 to 1999, she was a Researcher in the School of Radio Physics at the Kharkiv National University, and in 2000, a Royal Society—NATO Postdoctoral Fellow in the School of Electrical and Electronic Engineering, University of Nottingham, Nottingham, U.K., where she is currently a Research Fellow. Her research interests are in integral equation methods for electromagnetic wave scattering and eigenvalue problems, with applications to open waveguides, semiconductor microcavity lasers, and optical filters.



Trevor M. Benson (M'95–SM'01) was born in Sheffield, U.K., in 1958. He received the degree (first-class hon.) in physics and the Clark Prize in Experimental Physics and the Ph.D. degree in electronic and electrical engineering from The University of Sheffield, Sheffield, U.K., in 1979 and 1982, respectively.

After spending over six years as a Lecturer at University College Cardiff, Wales, U.K., he joined the University of Nottingham, Nottingham, U.K., as a Senior Lecturer in electrical and electronic engineering in 1989. He was promoted to the posts of Reader in Photonics in 1994 and Professor of Optoelectronics in 1996. His present research interests include experimental and numerical studies of electromagnetic fields and waves, with particular emphasis on propagation in optical waveguides and lasers, glass-based photonic circuits, and electromagnetic compatibility.

Prof. Benson has received the Electronics Letters and JJ Thomson Premiums from the Institute of Electrical Engineers (IEE), U.K. He is a Fellow of IEE, U.K., and the Institute of Physics.



Phillip Sewell (S'88–M'91–SM'04) was born in London, U.K., in 1965. He received the B.Sc. degree in electrical and electronic engineering and the Ph.D. degree (first class hon.) from the University of Bath, Bath, U.K., in 1988 and 1991, respectively.

From 1991 to 1993, he was an S.E.R.C. Postdoctoral Fellow at the University of Ancona, Ancona, Italy. Since 1993, he has been with the School of Electrical and Electronic Engineering, University of Nottingham, Nottingham, U.K. as Lecturer, Reader (from 2001), and Professor of Electromagnetics (from 2004). His research interests involve analytical and numerical modeling of electromagnetic problems, with application to optoelectronics, microwaves, and electrical machines.



Alexander I. Nosich (M'94–SM'95–F'04) was born in Kharkiv, Ukraine, in 1953. He received the M.Sc., Ph.D., and D.Sc. degrees in radio physics from the School of Radio Physics, Kharkov National University, Kharkov, Ukraine, in 1975, 1979, and 1990, respectively.

Since 1978, he has been with the Institute of Radio-Physics and Electronics (IRE), National Academy of Sciences of Ukraine, Kharkov, Ukraine, where he holds a post of Leading Scientist in the Department of Computational Electromagnetics. Since 1992, he has held research fellowships and visiting professorships in the EU, Turkey, Japan, and Singapore. His interests include methods of analytical regularization, free-space and open-waveguide scattering, complex mode behavior, radar cross section analysis, modeling of laser microcavities, and antenna simulation.